Synthesis and *in–vitro* anti–HIV–1 evaluation of novel pyrazolo[4,3–c]pyridin–4–one derivatives

Sanjay Kumar, Shiv Gupta, Leila Fotooh Abadi, Shraddha Gaikwad, Dipen Desai, Kamlesh Kumar Bhutani, Smita Kulkarni, Inder Pal Singh

PII: S0223-5234(19)30866-9

DOI: https://doi.org/10.1016/j.ejmech.2019.111714

Reference: EJMECH 111714

To appear in: *European Journal of Medicinal Chemistry*

Received Date: 27 December 2018

Revised Date: 23 August 2019

Accepted Date: 16 September 2019

Please cite this article as: S. Kumar, S. Gupta, L.F. Abadi, S. Gaikwad, D. Desai, K.K. Bhutani, S. Kulkarni, I.P. Singh, Synthesis and *in–vitro* anti–HIV–1 evaluation of novel pyrazolo[4,3–c]pyridin–4–one derivatives, *European Journal of Medicinal Chemistry* (2019), doi: https://doi.org/10.1016/j.ejmech.2019.111714.

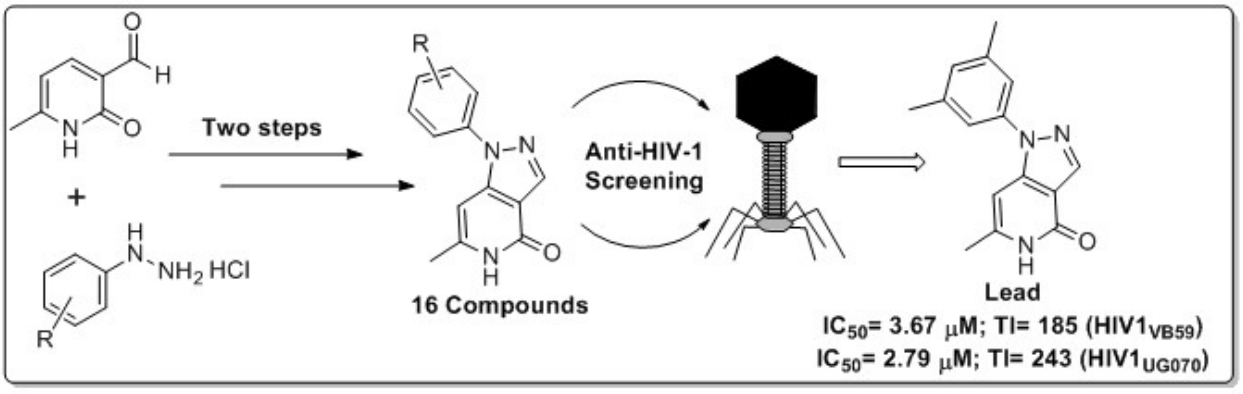

Synthesis and *In–vitro* Anti–HIV–1 Evaluation of Novel Pyrazolo[4,3–c]pyridin–4–one Derivatives

Sanjay Kumar[1], Shiv Gupta[1], Leila Fotooh Abadi[2], Shraddha Gaikwad[2], Dipen Desai[2], Kamlesh Kumar Bhutani[1#], Smita Kulkarni[2*], Inder Pal Singh[1*]

[1]*Department of Natural Products, National Institute of Pharmaceutical Education and Research (NIPER), Sector–67, S. A. S. Nagar–160 062, Punjab, India*

[2]*Department of Virology, ICMR–National AIDS Research Institute (NARI), Bhosari, Pune–411 026, Maharashtra, India*

*Address correspondence to this author at the Department of Natural Products, National Institute of Pharmaceutical Education & Research, S.A.S. Nagar, Punjab–160 062, India; Tel: +91–172–229–2144; Department of Virology, ICMR–National AIDS Research Institute (NARI), Bhosari, Pune–411 026, Maharashtra, India; Tel: +91–20–27331207/27331200; E–mails: ipsingh@niper.ac.in; ipsingh67@yahoo.com; skulkarni@icmr.org.in; skulkarni.nari@gov.in

25th December 1951 – 6th January 2018

ABSTRACT

In our continuing efforts to find novel anti–HIV compounds, we have synthesized sixteen novel pyrazolo[4,3–c]pyridin–4–one derivatives. All the synthesized compounds were screened for anti–HIV activity against HIV–1_{VB59} (R5, subtype C). Compounds **12a–12c** and **12e** were also tested against HIV–1_{UG070} (X4, subtype D) in TZM–bl cell line. Compound **12c** was found to be the most active against HIV–1_{VB59} and HIV–1_{UG070} with IC_{50} value 3.67 µM and 2.79 µM, and therapeutic indices 185 and 243, respectively. The lead compound **12c** inhibited the HIV-192/BR/018 (R5, subtype B) and drug resistant isolates, NIH-119 (X4/R5, subtype B) and NARI-DR (R5, subtype C) effectively. The activity of the lead compound was further confirmed by PBMC assays. The molecular docking data showed that the most active compound **12c** binds in the non-nucleoside binding pocket of HIV-1 reverse transcriptase, which was confirmed by the ToA assay. Thus the study indicated that **12c** may be considered as a NNRTI and further explored as a lead for anti-HIV drug development.

Key words: Pyrazolo[4,3–c]pyridin–4–one, Anti–HIV–1, QED, ADMET, TZM–bl.

1 INTRODUCTION

Acquired immunodeficiency syndrome (AIDS) is a result of advanced stage infection by human immunodeficiency virus (HIV). It is one of the world's most significant public health challenges, particularly in low– and middle–income countries. In 2017, approximately 36.9 million people (35.1 million adults) were living with HIV and 1.8 million people became newly infected, globally. Nearly 1 million people died from AIDS related illness in 2017 [1]. An estimated 21.7 million people were receiving HIV treatment in 2017. However, globally, only 59% of the 36.9 million people living with HIV were receiving antiretroviral therapy (ART). In 2017, 8 out of 10 pregnant women living with HIV received antiretrovirals (ARVs) to prevent and eliminate mother–to–child transmission and to keep mothers alive [2].

There are various antiretroviral drugs available in the market such as entry or fusion inhibitors, nucleoside or non–nucleoside reverse transcriptase inhibitors (NRTI/NNRTI), integrase inhibitors (IN), protease inhibitors (PI) and maturation inhibitors [3]. The resistance of virus to the available antiretroviral drugs is the biggest challenge for ART and the discovery of new anti–HIV agents to overcome this resistance is continually required.

Pyrazole is an important class of heterocyclic nucleus. Some of the pyrazole and fused–pyrazole containing drugs were approved for treatment of various diseases, including celecoxib (**1**) and lonazolac (**2**), COX–2 selective nonsteroidal anti–inflammatory drugs (NSAID) [4,5]; fipronil (**3**), an insecticide; dipyrone (**4**), a potent analgesic and antipyretic agent [6]; sildenafil (**5**) [7] used to treat erectile dysfunction (Figure 1).

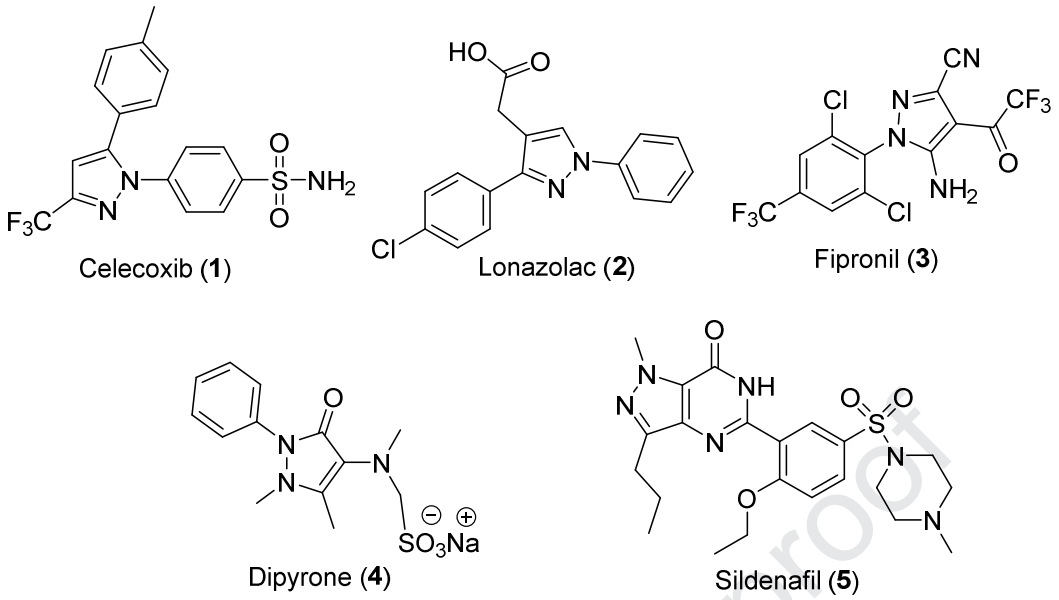

Figure 1. FDA approved pyrazole and fused–pyrazole containing drugs.

Fused–pyrazoles are reported for various biological activities including antiviral [8], antimicrobial [9,10], antiprotozoal [11], anticancer [12,13] and anti–inflammatory *etc* [14–16]. Some fused–pyrazole compounds were also reported for anti–HIV activity. The 1*H*–pyrazolo[3,4–b]pyridine–3–yl derivatives were reported for anti–HIV–1 activity, which were shown to act through reverse transcriptase inhibition [17,18] (Figure 2). Savant *et al*. reported novel 3–amino–4,5–dihydro–6–methyl–4–oxo–N–aryl–1*H*–pyrazolo[4,3–c]pyridine–7–carboxamide derivatives for anti–HIV activity against HIV–1 (IIIB) and HIV–2 (ROD) [19] (Figure 2). Here, we report sixteen new N–substituted 1*H*–pyrazolo[4,3–c]pyridine–4–one derivatives (Figure 3) and their evaluation for anti–HIV–1 activity. However, the N-substituted compounds are not yet known for these activities. The aim of this work was to evaluate the effect of introducing various N-substitutions on the fused pyrazolo-pyridine skeleton.

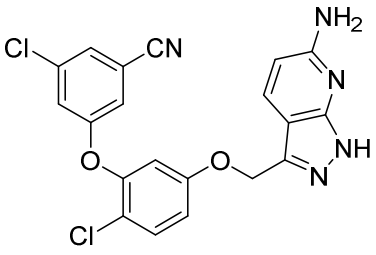

6 (MK-4965)
CIC_{95}= 8.4 nM (WT, 10% FBS)
CIC_{95}= 34 nM (WT, 50% NHS)

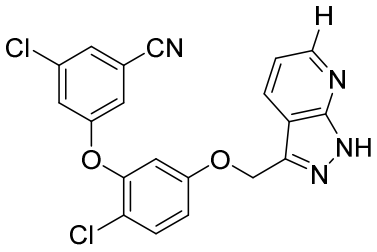

7
CIC_{95}= 10.3 nM (WT, 10% FBS)
CIC_{95}= 34 nM (WT, 50% NHS)

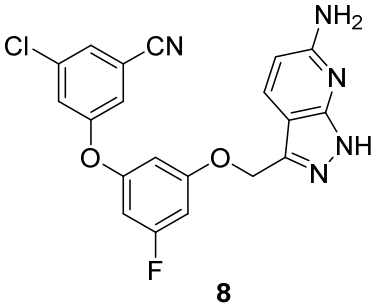

8
CIC_{95}= <3.8 nM (WT, 10% FBS)
CIC_{95}= 103 nM (WT, 50% NHS)

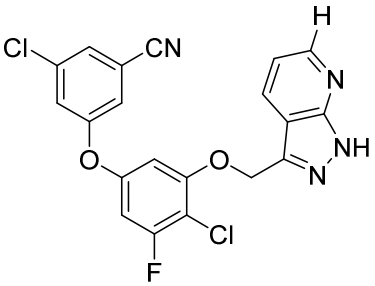

9
CIC_{95}= 11 nM (WT, 10% FBS)
CIC_{95}= 103 nM (WT, 50% NHS)

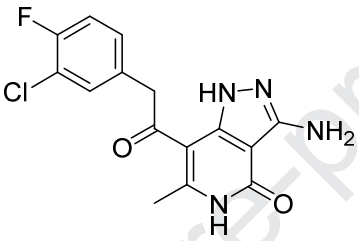

10
IC_{50}= 19.4 μM (HIV-1 IIIB)
IC_{50}= 14.4 μM (HIV-2 ROD)

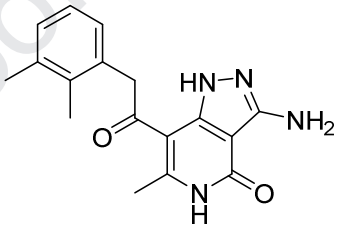

11
IC_{50}= 19.8 μM (HIV-1 IIIB)
IC_{50}= 19.0 μM (HIV-2 ROD)

CIC_{95} (cell culture inhibitory concentration): The concentration at which the spread of the virus is inhibited by >95%; WT: wild type; FBS: fetal bovine serum; NHS: normal human serum.

Figure 2. Synthetic fused–pyrazole derivatives for anti–HIV activity.

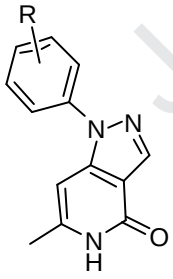

12a-12p
R = H, halogen, trifluoromethyl, alkyl

Figure 3. Structure of designed N–substituted 1*H*–pyrazolo[4,3–c]pyridine–4–one scaffold.

2 RESULTS AND DISCUSSIONS

2.1 *In silico* QED and ADMET properties

Drug–likeness assesses the oral bioavailability of a chemical compound in the early stages of drug discovery. Lipinski's rule of 5 along with other similar rules gives qualitative impression of drug–likeness. But these rules fail during the prioritization of chemicals based on their drug–likeness. Bickerton *et al.* addressed this problem and proposed Quantitative Estimation of Drug–likeness (QED) for the lead prioritization. They also suggested that compound with QED greater than 0.5 can be considered as a good lead for further drug development. In this work, sixteen new compounds were designed for synthesis by modifying the N-substituents and fused pyrazole ring and rationalized for their drug-like properties through *in silico* approach. QED of all designed compounds (**12a**– **12p**) was calculated according to the reported method (Table 1) [20]. In order to make comparison, QED value was calculated for two known drugs i.e. nevirapine (QED = 0.860) and zidovudine (QED= 0.422) [20–22]. QED value of all synthesized compounds was greater than 0.5, which indicated that the compounds possess drug-like properties.

Table 1. QED of pyrazolo[4,3–c]pyridin–4–one derivatives(**12a–12p**)

Compound No.	QED	Compound No	QED	Compound No	QED
12a	0.654	**12g**	0.687	**12m**	0.655
12b	0.634	**12h**	0.674	**12n**	0.672
12c	0.670	**12i**	0.693	**12o**	0.672
12d	0.670	**12j**	0.693	**12p**	0.717
12e	0.700	**12k**	0.694	Nevirapine	0.860
12f	0.687	**12l**	0.694	Zidovudine	0.420

All the compounds were further evaluated for *in silico* ADMET properties using admetSAR tool (Table 2) [23]. In order to validate the *in silico* protocol, we also evaluated *in silico* ADMET properties of two known drugs (nevirapine and zidovudine). The results indicated that, all the tested compounds along with nevirapine and zidovudine may cross blood brain barrier (BBB)

and absorb in human intestine (HIA) (Table 2). Results also showed all tested compounds along with nevirapine are permeable for Caco–2 cells, whereas, zidovudine showed negative result for Caco–2 cell permeability. The above predicted result for known drugs is also evident from the fact that zidovudine capsule and solution has oral bioavailability of less than 64% whereas oral bioavailability of nevirapine tablet was approximately 91% [24]. CYP450 isozymes are involved in the metabolism of drugs which in turn helps to excrete the drug out of the body and reduce the effect of the drug. These isozymes also play a major role in drug–drug interaction. All the tested compounds along with nevirapine were predicted as substrate for CYP450 3A4, whereas zidovudine is nonsubstrate for CYP450 3A4. The above results are in line with the literature reports that drug–drug interaction shown by nevirapine is due to the induction of CYP450 3A4 enzyme whereas zidovudine does not cause inhibition of CYP450 enzymes. Inhibition of CYP450 isozyme results in drug–drug interaction. Most of the designed compounds were found to be non–inhibitor of these enzymes. Compounds **12e, 12f** and **12g** were predicted to inhibit enzyme CYP450 1A2 and CYP450 2C19. All the tested compounds along with nevirapine and zidovudine were predicted to be non–inhibitors for enzymes CYP450 2C9, CYP450 2D6 and CYP450 3A4. The *in silico* results also showed these compounds are noncarcinogenic and nonmutagenic.

124 **Table 2.** *In silico* ADMET properties of designed pyrazolo[4,3–c]pyridin–4–one derivatives (**12a–12p**)

	12a	**12b**	**12c**	**12d**	**12e**	**12f**	**12g**	**12h**	**12i**	**12j**	**12k**	**12l**	**12m**	**12n**	**12o**	**12p**	**Nevirapine**	**Zidovudine**
BBB	+	+	+	+	+	+	+	+	+	+	+	+	+	+	+	+	+	+
HIA	+	+	+	+	+	+	+	+	+	+	+	+	+	+	+	+	+	+
Caco–2 permiability	+	+	+	+	+	+	+	+	+	+	+	+	+	+	+	+	+	–
P–GPS	NS	NS	NS	NS	NS	NS	NS	NS	NS	NS	NS	NS	NS	NS	NS	NS	NS	S
p–GPI	NI	NI	NI	I	I	NI	NI	NI	NI	NI	NI	NI	NI	I	I	I	NI	NI
Renal organic cation transport	NI	NI	NI	NI	NI	NI	NI	NI	NI	NI	NI	NI	NI	NI	NI	NI	NI	NI
CYP450 2C9 substrate	NS	NS	NS	NS	NS	NS	NS	NS	NS	NS	NS	NS	NS	NS	NS	NS	NS	NS
CYP450 2D6 substrate	NS	NS	NS	NS	NS	NS	NS	NS	NS	NS	NS	NS	NS	NS	NS	NS	S	NS
CYP450 3A4 substrate	S	S	S	S	S	S	S	S	S	S	S	S	S	S	S	S	S	NS
CYP450 1A2 inhibitor	NI	NI	NI	NI	I	I	I	I	I	I	I	I	I	I	I	I	I	NI
CYP450 2C9 inhibitor	NI	NI	NI	NI	NI	NI	NI	NI	NI	NI	NI	NI	NI	NI	NI	NI	NI	NI
CYP450 2D6 inhibitor	NI	NI	NI	NI	NI	NI	NI	NI	NI	NI	NI	NI	NI	NI	NI	NI	NI	NI
CYP450 2C19 inhibitor	NI	NI	NI	I	I	I	I	NI	NI	NI	NI	NI	NI	NI	NI	NI	NI	NI
CYP450 3A4 inhibitor	NI	NI	NI	NI	NI	NI	NI	NI	NI	NI	NI	NI	NI	NI	NI	NI	NI	NI

AMES Toxicity	NT	NT	NT	NT	NT	NT	NT	NT	NT	NT	NT	NT	NT	NT	NT	NT	T	T
Carcinogen	NC	NC	NC	NC	NC	NC	NC	NC	NC	NC	NC	NC	NC	NC	NC	NC	NC	NC

Blood–Brain Barrier (BBB): don't cross BBB (–); cross BBB (+), Human Intestinal Absorption (HIA): not absorbed (–); absorbed (+),Caco–2 Permeability: not permeable (–); permeable (+), Cytochrom 450 (CYP450): S = substrate for enzyme; NS = not a substrate for enzyme, I = enzyme inhibitor; NI = not enzyme inhibitor, NT: nontoxic; T: toxic, NC: noncarcinogenic.

2.2 Chemistry

All the designed compounds, a total of sixteen pyrazolo[4,3–c]pyridin–4–one derivatives were synthesized using Scheme 1. Compound 6–Methyl–2–oxo–1,2–dihydropyridine–3–carbonitrile (**14**) was synthesized using 3–ketobutyraldehyde dimethyl acetal (**13**) and cyanoacetamide as starting materials [25]. The nitrile group of compound **14** was then converted into formyl group using DIBAL–H to give compound **15** [26]. The structures of compounds **14** and **15** were confirmed by comparing melting point, ^{1}H NMR and ^{13}C NMR with the literature values [25,26]. The pyrazolo[4,3–c]pyridin–4–one derivatives were synthesized from compound **15** in two steps. In the first step, compound **15** and substituted phenylhydrazine hydrochlorides were stirred in ethanol at room temperature to yield intermediate hydrazones, which were used in second step without purification. Only one intermediate hydrazone, 6–methyl–3–((2–(*p*-tolyl) hydrazono) methyl) pyridin–2(1*H*)–one (**16a**) [22] obtained from the reaction of **15** with *p*–tolylhydazine hydrochloride was purified by repeated washing with ethanol for characterization. Spectral data of compound **16a** was matched with reported data [22]. In the second step, the intermediate hydrazones were converted in to pyrazolo[4,3–c]pyridin–4–one derivatives (**12a–12p**) in boiling nitrobenzene (Scheme 1) [27]. The structures of synthesized compounds (Figure 4) were confirmed by spectral data *i.e.* IR, mass, ^{1}H NMR, ^{13}C NMR *etc.* (Supplementary information).

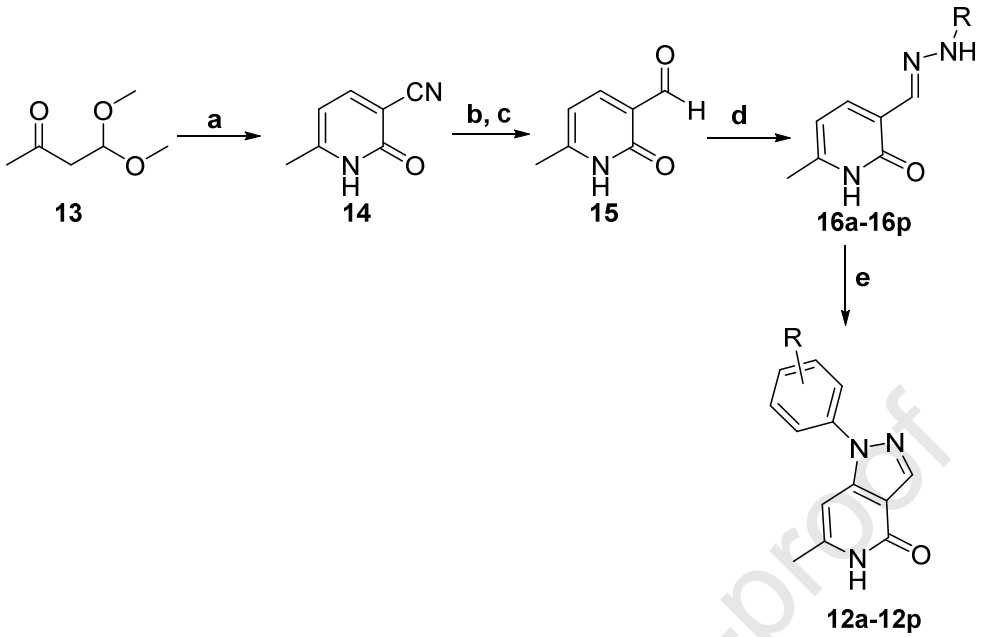

Scheme 1. (a) Cyanoacetamide, piperidine acetate, 80 °C, 24 h, 80%; b) HMDS, toluene, 110 °C, 3 h; c) DIBAL–H, toluene, 0 °C, 8 h, (combined yield of steps b and c: 75%); d) R–NH–NH_2.HCl, ethanol, rt, 2 h; e) Nitrobenzene, 210 °C, 15 min (combined yield of steps d and e: 41–64%).

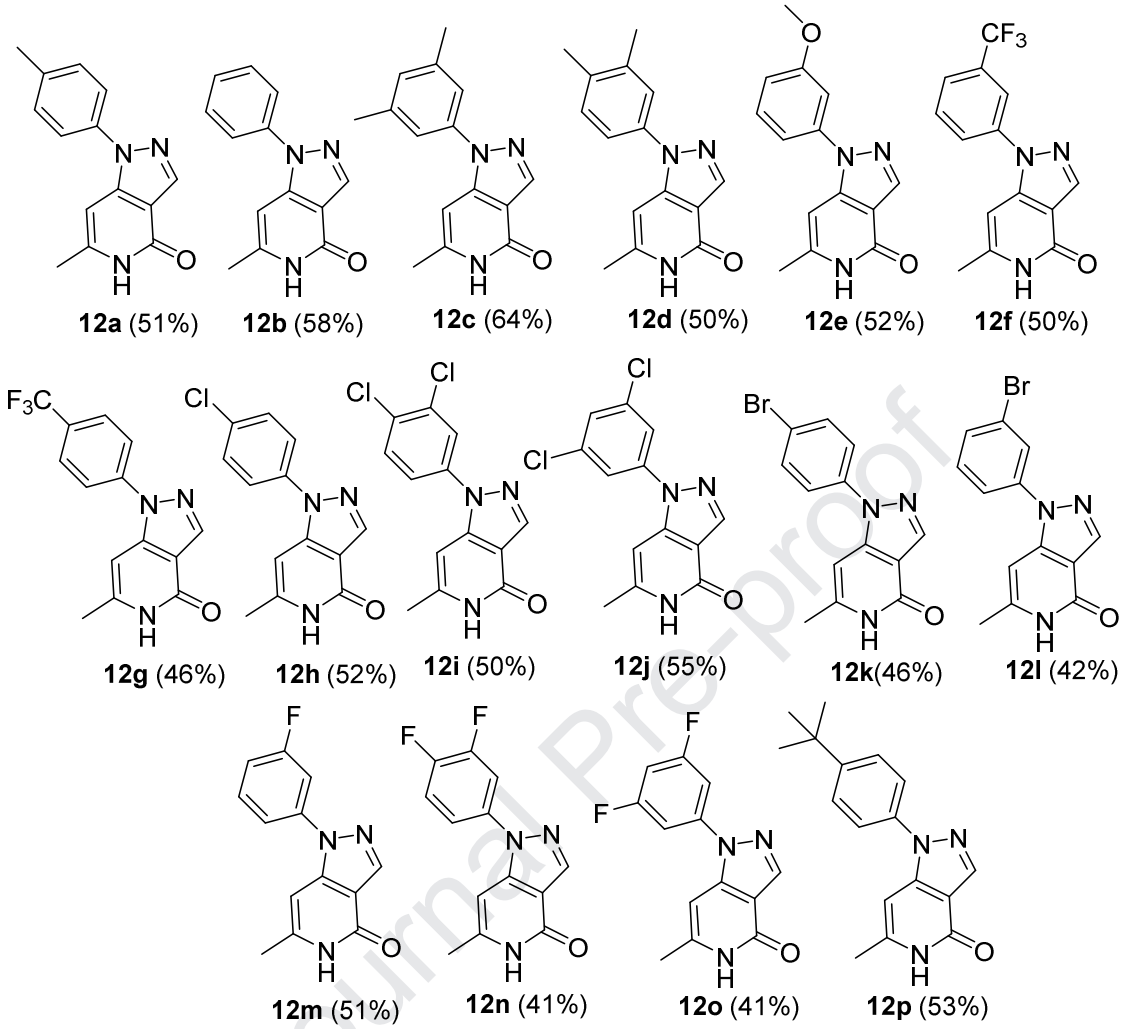

Figure 4. Structures of pyrazolo[4,3–c]pyridin–4–one derivatives (**12a–12p**).

2.3 Anti–HIV activity

Prior to screening the synthesized pyrazolo[4,3–c]pyridin–4–one derivatives (**12a–12p**) for anti–HIV activity, the compounds were tested for cytotoxicity using MTT cell viability assay and CC_{50} values were determined. The compound **12c** showed CC_{50} value 679 µM which is closer to CC_{50} value of Zidovudine *i.e.* 872 µM. Further all the compounds were screened for anti–HIV activity against HIV–1_{VB59} (R5, subtype C). The compounds **12a**–**12d** and **12e** were further tested against both HIV–1_{VB59} (R5, subtype C) and HIV–1_{UG070} (X4, subtype D) in TZM–bl cell

158 line. The compounds **12d** and **12f**–**12p** were not tested against HIV–1_{UG070} (X4, subtype D)
159 because of IC_{50} of these compounds against HIV–1_{VB59} (R5, subtype C) was less than CC_{50}
160 value. The IC_{50} values and therapeutic indices (TI) were calculated for each of them and
161 compared with the drug control (Table 3). The compound **12c** was the most active compound
162 against HIV–1_{VB59} and HIV–1_{UG070} among all the tested pyrazolo[4,3–c]pyridin–4–one
163 derivatives showing IC_{50} values of 3.67 µM and 2.79 µM, respectively, against these two strains.
164 The compound **12c** also showed good therapeutic indices 185 and 243 against HIV–1_{VB59} and
165 HIV–1_{UG070}, respectively. Subsequently, the active lead compound **12c** was also tested against
166 HIV-$1_{92/BR/018}$ (R5, subtype B) and exhibited IC_{50} value7.42±2.3 µM. Furthermore, the compound
167 was also effective against two nevirapine drug resistant isolates HIV-1_{N119} (X4/R5, subtype B)
168 and HIV-$1_{NARI-DR}$ (R5, subtype C) with IC_{50} values 3.24±0.9 µM and 2.53±0.2 µM, respectively
169 (Table 4).
170 Substitutions of N–1 phenyl ring with electron withdrawing groups like –F, –Cl, $–CF_3$ and –
171 OCH_3 lead to loss of the anti–HIV activity, whereas, substitution with methyl group leads to
172 increased anti–HIV activity. Further, compound **12c** with 3,5–dimethyl substitution possessed
173 greater anti–HIV activity as compared to the 4–methyl and 3,4–dimethyl substituted compounds.
174 Similarly, substitutions of N–1 phenyl ring with electron withdrawing groups like –F, –Cl, $–CF_3$
175 and $–OCH_3$ resulted in increased toxicity and substitution with methyl ring led to reduced
176 toxicity.
177
178
179
180

Table 3. Anti–HIV–1 activity of pyrazolo[4,3–c]pyridin–4–one derivatives (**12a–12p**)

Sr. No	Compound No.	Cytotoxicity CC_{50} (µM)	Anti–HIV–1 testing data			
			IC_{50} $HIV1_{VB59}$ (R5) (µM)	TI $HIV1_{VB59}$ (R5)	IC_{50} $HIV1_{UG070}$ (X4) (µM)	TI $HIV1_{UG070}$ (X4)
1	**12a**	383.18	58.08	6.6	228.79	1.67
2	**12b**	708.00	120.80	5.86	444.44	NA
3	**12c**	679.00	3.67	185	2.79	243
4	**12d**	93.40	126.44	0.74	NT	NT
5	**12e**	552.94	246.78	2.24	>196.08	NA
6	**12f**	34.06	127.78	1.00	NT	NT
7	**12g**	100.35	>170.65	NA	NT	NT
8	**12h**	260.25	>193.05	NA	NT	NT
9	**12i**	93.50	>170.65	NA	NT	NT
10	**12j**	93.50	>170.65	NA	NT	NT
11	**12k**	79.80	138.28	0.58	NT	NT
12	**12l**	72.57	139.47	0.52	NT	NT
13	**12m**	158.72	>205.76	NA	NT	NT
14	**12n**	133.45	>191.57	NA	NT	NT
15	**12o**	129.54	>191.57	NA	NT	NT
16	**12p**	45.91	>177.94	NA	NT	NT
17	**Zidovudine**	872	0.03	29067	0.027	32296

CC_{50}: 50% cytotoxic concentration; IC_{50}: 50% inhibitory concentration; Therapeutic index (TI): CC_{50}/IC_{50}; NA: Not applicable; NT: Not tested

Table 4. Anti–HIV–1 activity of lead compound **12c** against various primary isolates of HIV-1

Comp.	CC_{50} (µM)	HIV-1 primary isolates									
		HIV-1 $_{VB59}$		HIV-1 $_{UG070}$		HIV-1 $_{92/BR/018}$		HIV-1 $_{NARI-DR}$		HIV-1_{N119}	
		IC_{50} (µM)	TI	IC_{50} (µM)	TI	IC_{50} (µM)	TI	IC_{50} (µM)	TI	IC_{50} (µM)	TI
12c	679 ±223	3.67 ±2.3	185	2.79 ±1.8	243	7.42 ±2.3	91	2.53 ±0.2	268	3.24 ±0.9	210
Zidovudine	872± 13.8	0.02± 0.01	43600	0.01± 0.0	87200	0.016± 0.005	54500	0.02± 0.01	43600	0.02± 0.01	43600
Nevirapine	597 ±63	0.71 ±0.1	840	0.53 ±0.3	1126	0.30 ±0.1	1990	232.3 ±13.7	2.6	140.0 ±52.6	4.3

CC_{50}: 50% cytotoxic concentration; IC_{50}: 50% inhibitory concentration; Therapeutic index (TI): CC_{50}/IC_{50}

The data represents Mean ± SD of three independent assays.

The lead compound **12c** exhibited a CC_{50} of 592 µM and IC_{50} value of 8.65 µM in the confirmatory assays carried out in PBMCs against HIV–1_{VB51} (Table 5). Compounds **12a** and **12c** were also tested for the inhibition of reverse transcriptase (RT) enzyme. Compound **12c** exhibited an IC_{50} value 30.80±9.65 µM, while compound **12a** had an IC_{50} value of 82.90±5.58 µM . Zidovudine and Nevirapine were used as controls in the assay and inhibited the HIV–1 RT with an IC_{50} of 0.02 ± 0.01 µM and 13.14±1.88 µM, respectively.

Table 5. Anti–HIV–1 activity of **12c** in PBMCs

Sr. No	Compound No.	Average Cytotoxicity CC_{50} ((µM)	Anti–HIV–1 testing data	
			IC_{50} $HIV1_{VB51}$ (R5) (µM)	TI $HIV1_{VB51}$ (R5)
1	**12c**	592±124	8.65±2.09	68
2	**Zidovudine**	1071±25	0.05±0.01	21420
3	**Nevirapine**	1003±16	0.19±0.03	5278

CC_{50}: 50% cytotoxic concentration; IC_{50}: 50% inhibitory concentration; Therapeutic index (TI) = CC_{50}/IC_{50}.

2.3.1: Time-of addition experiment

To identify the target of the drug action, the time-of-addition assay (ToA) was carried out using the lead compound **12c** along with known anti-retrovirals (ARVs). It was observed that the inhibition of the lead compound **12c** declined after 10 h post infection similar to NVP (Figure 5).

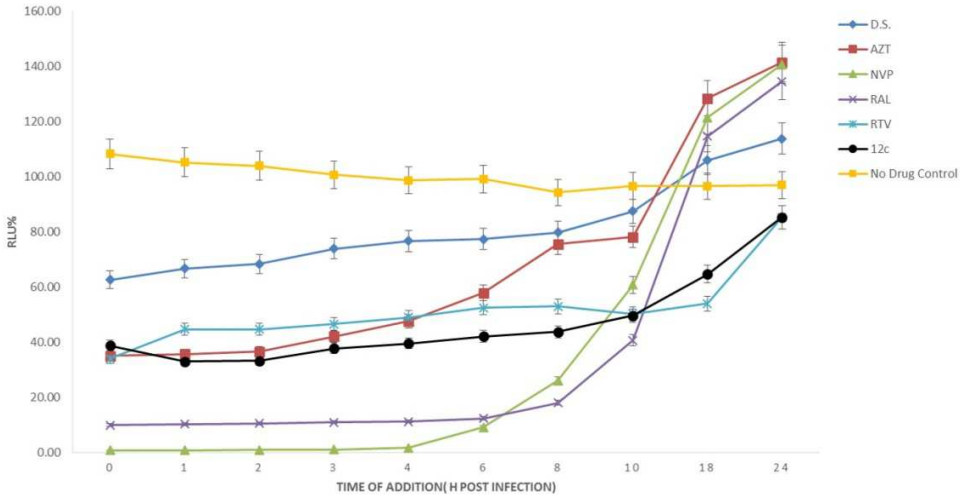

Figure 5. Time-of-addition analysis.

The target of lead compound **12c** was compared to known antiretroviral drugs. Final compound concentrations were 5-fold higher than their IC_{50} values. D.S. (0.25 μg/mL), AZT (0.05 μM), NVP (0.94 μM), RAL (0.16 μM), RTV (59.39 μM) and **12c** (1.42 μM). Test compounds were added at different time points (0, 1, 2, 3, 4, 6, 8, 10, 18, and 24 h) at or after infection. The percent infection (RLU) was determined. Data represent mean±SD calculated from three independent experiments. The results showed that **12c** followed an inhibition pattern similar to AZT upto 3 h which continued up to 10 h like NVP. It was noted that the activity of compound **12c** depended on the concentration tested. It blocked the viral reverse transcription process at low concentrations, whereas, at higher concentrations, it showed inhibition for extended duration. Thus the ToA assay enabled to discriminate between NRTI versus NNRTI.

2.4 Molecular docking

Blind docking calculations were carried out to find the potential binding sites of **12c** in the reverse transcriptase enzyme. The results showed that **12c** binds within 48 pockets of the reverse transcriptase (Figure 6). The highest energy cluster (-10.5 kcal/mol) of **12c** occupies the allosteric binding site of non-nucleoside reverse transcriptase inhibitors. Further, docking studies of all the synthesized compounds (**12a–12p**) were performed within the non-nucleoside binding pocket (NNBP) to study the binding modes. The binding mode analysis showed that the phenyl ring of **12a**, **12b**, **12d–12l** and **12n–12p** (Figure 7a) and pyridinone ring of compounds **12c** and **12m** (Figure 7b) occupies the aromatic-rich region of NNBP. Interestingly, **12f** and **12c** showed maximum binding affinities of -10.9 and -10.5 kcal/mol, respectively (Table 6). The binding affinity of **12c** is translated into the anti-HIV activity contrary to **12f**. The analysis of the protein-

ligand interaction showed that the pyridinone moiety of **12c** occupies a hydrophobic aromatic-rich pocket formed mainly by the side chains of Tyr181, Tyr188, Phe227, and Trp229. The hydrophobic contacts were found between the pyridinone ring of **12c** and residue Y181 and Y188 (Figure 8b). These hydrophobic interactions were absent in **12f** (Figure 8a). Furthermore, the phenyl ring of **12f** occupies the hydrophobic pocket formed by the side chains of Tyr181, Leu100. The hydrogen bonding in **12f** increases the binding affinity but in effect, it reduces the hydrophobic interactions with residue Y181 and Y188 (Figure 8a). Compound **12m** also interacts with the residue Y181 and Y188 but its binding affinity (-9.5 kcal/mol) is low. No other compound showed interaction with both of the residues *i.e* Y181 and Y188. The NNBP does not exist in the absence of an inhibitor; rather, binding of these inhibitors causes the side chains of Y181 and Y188 to flip from a ‘down’ to an ‘up’ orientation which generates this NNBP [28]. Therefore, the interaction of inhibitors with these residues is considered important for the activity. These results support the hypotheses about the importance of hydrophobic contacts for NNBP.

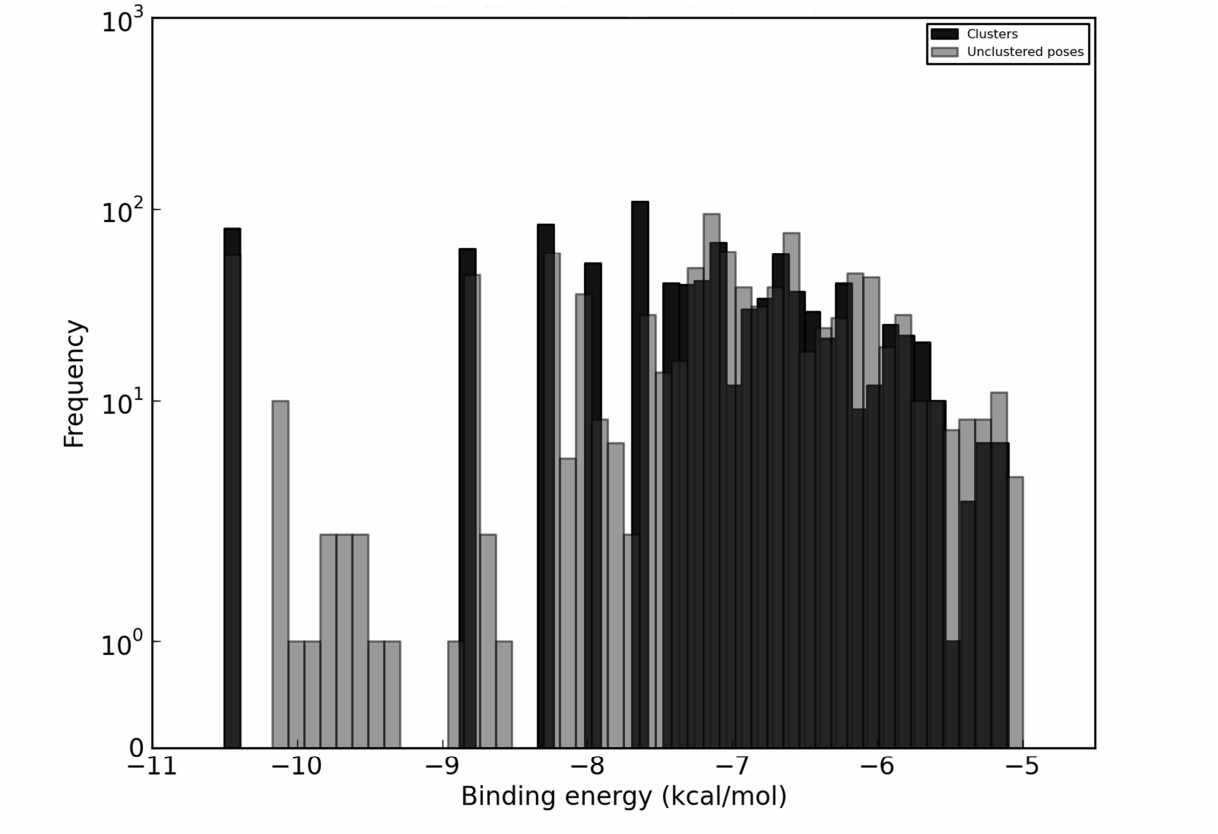

Figure 6. Clustered blind docking results.

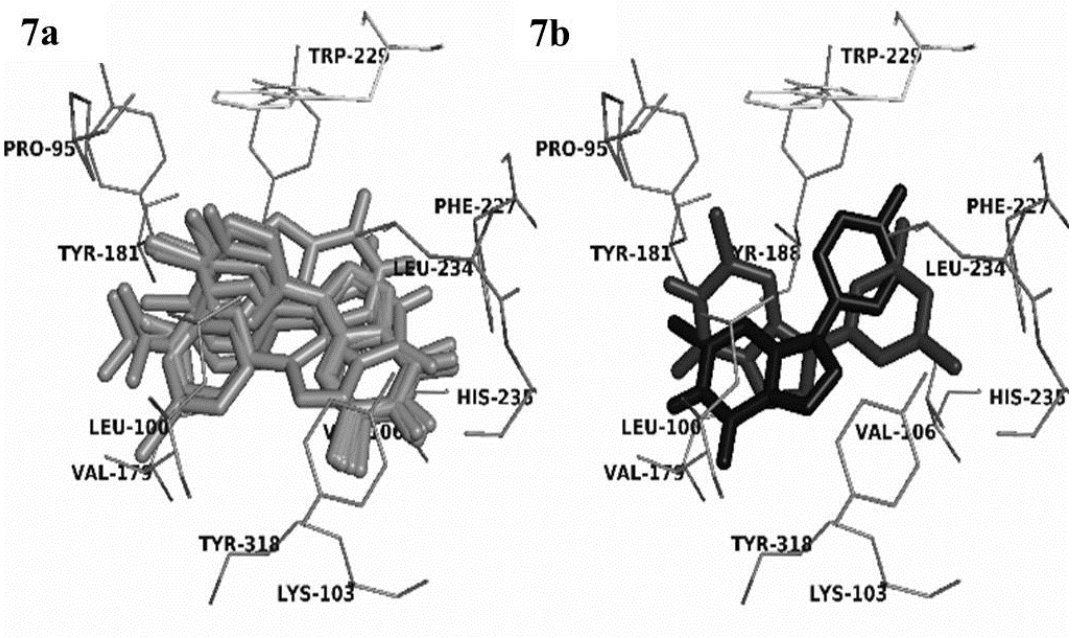

Figure 7. Binding mode of compounds **12a**–**12p** a) Compound **12a**, **12b**, **12d**–**12l** and **12n**–**12p** b) Compound **12c** and **12f** .

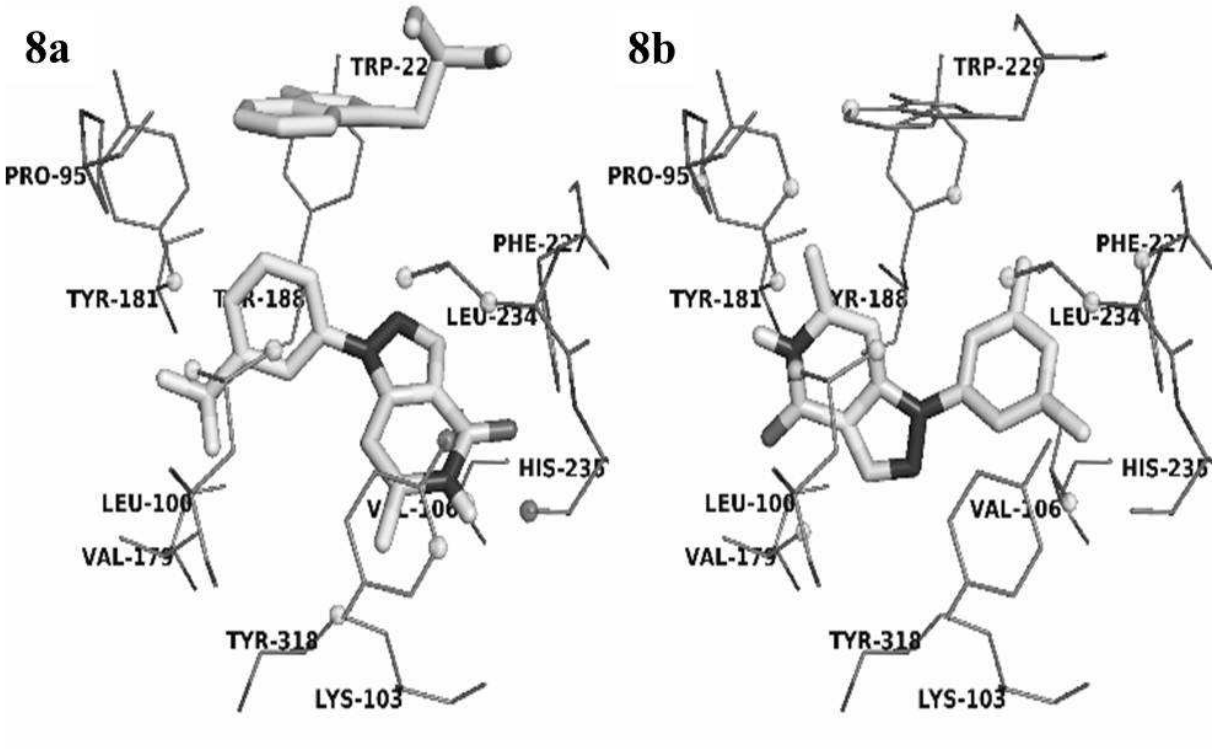

Figure 8. Binding modes of **12f** (8a) and **12c** (8b) showing various interactions with reverse transcriptase enzyme (Atoms of protein involved in hydrophobic interactions are shown as grey ball and atoms of protein involved in hydrogen bond are shown as black ball. Residue involved in pi-stacking is shown as grey stick).

Table 6. Binding affinities and interactions of compounds **12a–12p**

Compound	Binding Affinity (kcal/mol)	Hydrophobic interaction	Hydrogen Bond	pi-Stacking	Halogen Bond
12a	-9.8	P95, L100, K103, V106, Y181, L234, Y318	H235, Y318	W229	–
12b	-9.6	L100, K103, V106, Y181, Y318	H235, Y318	W229	–
12c	-10.5	P95, L100, V106, V179, Y181, Y188, F227, W229, L234	–	–	–
12d	-10.3	P95, L100, K103, V106, Y181, L234, Y318	H235, Y318	W229	–
12e	-9.7	L100, K103, V106, Y181, Y318	H235, Y318	W229	–
12f	-10.9	L100, K103, V106, Y181, L234, Y318	H235, Y318	W229	–
12g	-10.4	V106, V179, Y181, F227	Y318	W229	–
12h	-9.7	L100, K103, V106, L234,	H235, Y318	W229	–

		Y318			
12i	-10.1	L100, K103, V106, L234, Y318	H235, Y318	W229	–
12j	-9.6	L100, K103, V106, Y181, L234, Y318	P236, Y318	–	V179
12k	-9.3	L100, V106, V179, Y181, F227, L234	–	W229	–
12l	-10.1	L100, K103, V106, Y181, L234, Y318	H235, Y318	W229	–
12m	-9.5	L100, V106, Y181, Y188, F227, L234	K101	W229	–
12n	-10.3	L100, K103, V106, Y318	H235, Y318	W229	–
12o	-10	L100, K103, V106, Y181, L234, Y318	H235, Y318	W229	–
12p	-10	L100, K103, V106, Y181, L234, Y318	H235, Y318	W229	–

3 CONCLUSIONS

Sixteen new pyrazolo[4,3–c]pyridin–4–one derivatives were synthesized. All synthesized compounds were predicted to be drug-like as indicated by QED value greater than 0.5. Also, synthesized compounds were predicted to have favorable ADMET parameters. Compound **12c** was found to be the most active against HIV–1_{VB59} and HIV–1_{UG070} with IC_{50} value 3.67 µM and 2.79 µM, and therapeutic indices of 185 and 243, respectively. The compound could also inhibit nevirapine drug resistant viruses and has been shown to inhibit reverse transcriptase assay. The molecular docking study showed that the most active compound **12c** binds in the non-nucleoside binding pocket of HIV–1 reverse transcriptase, which was confirmed by ToA assay. The study indicated that **12c** may be considered as a NNRTI can be further explored as a lead for anti–HIV–1 drug development.

4 EXPERIMENTAL

4.1 General

All chemicals were purchased from Sigma–Aldrich, Hyderabad, India, or Alfa Aeser, Hyderabad, India, and used without further purification for the synthesis of pyrazolo[4,3–c]pyridin–4–one derivatives. Solvents used for the synthesis were of LR (laboratory reagent) grade and used without further purification. Precoated silica gel aluminum sheets (TLC Silica gel 60 F_{254}, 0.25 mm thickenss, Merck, Germany) were used for TLC and visualized under UV light and derivatized using Dragendorff reagent. Compounds were purified using Silica gel (#230–400, Merck, Germany) column chromatography. Purity of synthesized compounds was checked using high–performance liquid chromatography (HPLC, Shimadzu Corporation, Kyoto, Japan).

All the newly synthesized pyrazolo[4,3–c]pyridin–4–one derivatives were characterized by using by ^{1}H NMR, ^{13}C NMR, mass spectrometer and High–Resolution Mass Spectra (HRMS). ^{1}H NMR and ^{13}C NMR spectra were recorded on 400 and 100 MHZ (Bruker FT–NMR Avance II, USA) spectrometer, respectively, using tetramethylsilane as an internal standard. The chemical shifts are reported in δ units. Melting points were recorded on capillary melting point apparatus (Buchi). Infra–red (IR) spectra were recorded by using Perkin Elmer–Spectrum II instrument. Mass spectra were recorded on Thermo LTQ–XL mass spectrometer (Thermo, USA). HRMS were recorded on maxis^{TM} ESI–Q–TOF (Bruker, Germany).

4.2 Synthesis of 6–methyl–2–oxo–1,2–dihydropyridine–3–carbonitrile (14)

The compound **14** was synthesized using a method reported by Walton *et al.* [25]. 3–Ketobutyraldehyde dimethyl acetal (**13**) (38 mmol, 5.0 g, 5 mL) and cyanoacetamide (41.8 mmol, 3.52 g) were mixed in 250 mL round bottom flask (RBF). The piperidinium acetate solution (25% v/v, 15 mL) was added with stirring to dissolve the mixture. The resulted reaction

mixture was transferred at 80 °C and stirred continuously for 24 h. The reaction mixture was cooled to room temperature and filtered to collect the precipitate, which was washed with cold water three times and dried under vacuum to give white compound **14** (3.7 g, 73 % yield) (Scheme 1).

4.3 Synthesis of 6–methyl–2–oxo–1,2–dihydropyridine–3–carbaldehyde (15)

Compound **15** was synthesized using the method described by Showalter *et al.* [26]. In brief, compound **14** (14.9 mmol, 2 g) and hexamethyldisilazane (14.9 mmol, 2.4 g, 3.1 mL) were mixed in 100 mL round bottom flask (RBF) under nitrogen. To above mixture, dry toluene (10 mL) was added and mixture was stirred at 120 °C for 2 h to give clear solution. The reaction mixture was cooled to room temperature followed by removal of the solvent under vacuum to obtain yellowish oil. Dry toluene (30 mL) was added to the oily residue under nitrogen with continuous stirring at 0 °C. Di-isobutylaluminium hydride (DIBAL–H) (25% w/w in toluene) (14 mL) was added dropwise for 1 h to above solution. The reaction mixture was stirred at 0 °C for 8 h. After completion, the reaction solution was transferred in to 250 mL RBF and acidified with 3N HCl (50 mL) to give yellow precipitate. The reaction mixture was extracted with the dichloromethane (DCM) three times. Combined DCM extract was treated with activated charcoal and concentrated under vacuum after filtration to give yellowish compound **14** (1.7 g, 82 % yield) (Scheme 1).

4.4 Synthesis of pyrazolo[4,3–c]pyridin–4–one derivatives (12a–12q)

The pyrazolo[4,3–c]pyridin–4–one derivatives were synthesized by using compound **15** as starting material in two steps. In first step, the compound **15** (1 mmol, 137 mg) was dissolved in ethanol (20 mL) and substituted phenylhydrazine hydrochloride (1.1 equivalent) was added. The reaction mixture was stirred at room temperature for 2 h. The completion of reaction was

monitored by TLC. The resulted reaction mixture was allowed to cool to room temperature. The solvent was evaporated under vacuum; ethanol (5 mL) was added and sonicated for 30 seconds to produce suspension. The resulted suspensions were kept in refrigerator for 1 h to settle down the suspended particles. The suspended particles was filtered out and used for second step without further purification. In second step, the resulted solid was poured in boiling nitrobenzene at 210 °C and stirred at same temperature for 15 minutes [27]. The completion of reaction was monitored by TLC. After the completion, the reaction mixture was allowed to cool to room temperature followed by silica gel column chromatography to isolate pure pyrazolo[4,3–c]pyridin–4–one derivatives (**12a–12p)**.

6–Methyl–1–(*p*–tolyl)–1*H*–pyrazolo[4,3–c]pyridin–4(5*H*)–one (**12a**): Light brown solid; Yield 51%; mp = 263–265 °C; FTIR ($CHCl_3$) υ cm^{-1}3418,2923, 2851, 1673, 1463, 1377; ^{1}H NMR ($CDCl_3$, 400 MHz): δ 11.46 (s, 1H), 8.31 (s, 1H), 7.49 (d, J = 7.0 Hz, 2H), 7.33 (d, J = 6.9 Hz, 2H), 6.36 (s, 1H), 2.44 (s, 6H); ^{13}C NMR ($CDCl_3$, 100 MHz): δ 161.0, 144.7, 142.5, 137.9, 137.5, 136.7, 130.1 (2C), 123.3 (2C), 112.5, 92.2, 21.1, 19.6; HRMS (ESI) *m/z* cacld for $C_{14}H_{13}N_3O$ $[M+Na]^+$: 262.0956, found: 262.0944.

6–Methyl–1–phenyl–1*H*–pyrazolo[4,3–c]pyridin–4(5*H*)–one (**12b**): Tint white solid; Yield 58%; mp = 236–240 °C; FTIR ($CHCl_3$) υ cm^{-1} 3443,2922, 2851, 1651, 1458, 1377, 758; ^{1}H NMR ($CDCl_3$, 400 MHz): δ 11.30 (s, 1H), 8.33 (s, 1H), 7.62 (dd, J = 8.6, 1.1 Hz, 2H), 7.57–7.53 (m, 2H), 7.43 (t, J = 7.4 Hz, 1H), 6.41 (s, 1H), 2.44 (s, 3H); ^{13}C NMR ($CDCl_3$, 100MHz): δ 161.0, 148.4, 144.7, 142.7, 139.1, 137.7, 129.6 (2C), 127.9, 123.4 (2C), 112.7, 92.3, 19.7; HRMS (ESI) *m/z* cacld for $C_{13}H_{11}N_3O$ $[M+Na]^+$: 248.0800, found: 248.0792.

1–(3,5–Dimethylphenyl)–6–methyl–1*H*–pyrazolo[4,3–c]pyridin–4(5*H*)–one (**12c**): White solid; Yield 64%; mp = 286–289 °C; FTIR ($CHCl_3$) υ cm^{-1} 3432,2917, 1633, 1459, 1259, 749;

^{1}H NMR ($CDCl_3$, 400 MHz): δ 11.46 (s, 1H), 8.31 (s, 1H), 7.22 (s, 2H), 7.06 (s, 1H), 6.38 (s, 1H), 2.45 (s, 3H), 2.41 (s, 6H); ^{13}C NMR ($CDCl_3$, 100 MHz): δ 161.1, 144.7, 142.5, 139.5, 139.0, 137.4, 129.5 (2C), 121.2 (2C), 112.5, 92.4, 21.3 (2C), 19.7; HRMS (ESI) *m/z* cacld for $C_{15}H_{15}N_3O$ $[M+Na]^+$: 276.1113, found: 276.1104.

1–(3,4–Dimethylphenyl)–6–methyl–1*H*–pyrazolo[4,3–c]pyridin–4(5*H*)–one (**12d**): Brown solid; Yield 50%; mp = 248–250 °C; FTIR ($CHCl_3$) υ cm^{-1} 3433,2923, 1638, 1459, 1016; ^{1}H NMR ($CDCl_3$, 400 MHz): δ 11.36 (s, 1H), 8.30 (s, 1H), 7.39 (d, J = 1.9 Hz, 1H), 7.31 (dd, J = 8.1, 2.0 Hz, 1H), 7.29 (s, 1H), 6.36 (s, 1H), 2.43 (s, 3H), 2.36 (s, 3H), 2.34 (s, 3H); ^{13}C NMR ($CDCl_3$, 100 MHz):161.0, 144.7, 142.4, 138.2, 137.4, 136.9, 136.6, 130.4, 124.7, 120.7, 112.5, 92.3, 19.9, 19.7, 19.5; HRMS (ESI) *m/z* cacld for $C_{15}H_{15}N_3O$ $[M+Na]^+$: 276.1113, found: 276.1105.

1–(3–Methoxyphenyl)–6–methyl–1*H*–pyrazolo[4,3–c]pyridin–4(5*H*)–one (**12e**): Brown solid; Yield 52%; mp = 184–189 °C; FTIR ($CHCl_3$) υ cm^{-1} 3433,2923, 1638, 1466, 1017; ^{1}H NMR ($CDCl_3$, 400 MHz): δ 10.99 (s, 1H), 8.31 (s, 1H), 7.44 (m, 1H), 7.20–7.18 (m, 2H), 6.97 (m, 1H), 6.43 (s, 1H), 3.89 (s, 3H), 2.43 (s, 3H); ^{13}C NMR ($CDCl_3$, 100 MHz): δ 160.6, 144.7, 142.6, 140.2, 137.7, 130.2, 115.4, 113.7, 109.2, 106.3, 101.5, 92.4, 55.6, 19.7; HRMS (ESI) *m/z* cacld for $C_{14}H_{13}N_3O_2$ $[M+Na]^+$: 278.0905, found: 278.0895.

6–Methyl–1–(3–(trifluoromethyl)phenyl)–1*H*–pyrazolo[4,3–c]pyridin–4(5*H*)–one (**12f**): Light brown solid; Yield 50%; mp = 233–235 °C; FTIR ($CHCl_3$) υ cm^{-1} 3390,2921, 2850, 1671, 1465, 1275, 1120, 750; ^{1}H NMR ($CDCl_3$, 400 MHz): δ 11.52 (s, 1H), 8.36 (s, 1H), 7.93 (s, 1H), 7.84 (m, 1H), 6.69 (m, 2H), 6.40 (s, 1H), 2.48 (s, 3H); ^{13}C NMR ($CDCl_3$, 100 MHz): δ 160.9, 144.7, 143.5, 139.7, 138.4, 132.1, 130.3, 126.2, 124.8, 124.4, 120.2, 114.1, 91.8, 19.8; MS (ESI) *m/z* 294 [M + 1], 316 $[M+Na]^+$ for $C_{14}H_{10}F_3N_3O$.

6–Methyl–1–(4–(trifluoromethyl)phenyl)–1*H*–pyrazolo[4,3–c]pyridin–4(5*H*)–one (**12g**): Brown solid; Yield 46%; mp = 262–264 °C; FTIR ($CHCl_3$) υ cm^{-1} 3435, 2920, 2851, 1669, 1330, 1108, 1062; ^{1}H NMR ($CDCl_3$, 400 MHz): δ 10.97 (s, 1H), 8.35 (s, 1H), 7.83–7.78 (m, 4H), 6.44 (s, 1H), 2.45 (s, 3H); ^{13}C NMR ($CDCl_3$, 100 MHz):δ 160.6, 144.8, 143.3, 142.0, 138.5, 129.5, 126.9 (2C), 123.1 (2C), 122.4, 113.2, 91.9, 19.8; MS (ESI) *m/z* 294 [M+H], 316 $[M+Na]^+$ for $C_{14}H_{10}F_3N_3O$.

1–(4–Chlorophenyl)–6–methyl–1*H*–pyrazolo[4,3–c]pyridin–4(5*H*)–one (**12h**): Light brown solid; Yield 52%; mp = 247–249 °C; FTIR ($CHCl_3$) υ cm^{-1} 3433, 2955, 2922, 2852, 1663, 1461, 1377, 1262, 751; ^{1}H NMR ($CDCl_3$, 400 MHz): δ 10.88 (s, 1H), 8.31 (s, 1H), 7.58–7.50 (m, 4H), 6.36 (s, 1H), 2.42 (s, 3H); ^{13}C NMR ($CDCl_3$, 100 MHz): 156.3, 144.7, 142.8, 138.0, 137.7, 134.7, 133.6, 129.8 (2C), 124.5 (2C), 114.9, 92.0, 19.7; HRMS (ESI) *m/z* cacld for $C_{13}H_{10}ClN_3O$ $[M+Na]^+$: 282.0410, found: 282.0404.

1–(3,4–Dichlorophenyl)–6–methyl–1*H*–pyrazolo[4,3–c]pyridin–4(5*H*)–one (**12i**): Light brown solid; Yield 50%; mp = 273–275 °C; FTIR ($CHCl_3$) υ cm^{-1} 3435, 2919, 2850, 1634, 1487, 750; ^{1}H NMR (DMSO–d_6, 400 MHz): δ 11.35 (s, 1H), 8.27 (s, 1H), 7.93 (d, J = 2.2 Hz, 1H), 7.83 (d, J = 8.7 Hz, 1H), 7.69 (dd, J = 8.7, 2.3 Hz, 1H), 6.55 (s, 1H), 2.26 (s, 3H); ^{13}C NMR (DMSO–d_6, 100 MHz): δ 159.1, 144.9, 139.0, 138.6, 132.6, 132.0, 130.4, 125.0, 123.3, 113.2, 91.2, 79.5, 19.4; MS (ESI) *m/z* 294 $[M+H]^+$, 296 $[M+2+H]^+$, 298 $[M+4+H]^+$, 316 $[M+Na]^+$, 318 $[M+2+Na]^+$, 320 $[M+4+Na]^+$ for $C_{13}H_9Cl_2N_3O$.

1–(3,5–Dichlorophenyl)–6–methyl–1*H*–pyrazolo[4,3–c]pyridin–4(5*H*)–one (**12j**): Light brown solid; Yield 55%; mp = 242–244 °C; FTIR ($CHCl_3$) υ cm^{-1}3435, 2920, 2850, 1671, 1460, 766; ^{1}H NMR (DMSO–d_6, 400 MHz): δ 11.38 (s, 1H), 8.28 (s, 1H), 7.74 (s, 2H), 7.72 (s, 1H), 6.56 (s, 1H), 2.28 (s, 3H); ^{13}C NMR (DMSO–d_6, 100 MHz): δ 159.0, 145.1, 145.0, 141.2, 138.8,

135.4 (2C), 127.6, 121.9 (2C), 113.3, 91.2, 19.4; MS (ESI) *m/z* 294 $[M+H]^+$, 296 $[M+2+H]^+$, 298 $[M+4+H]^+$, 316 $[M+Na]^+$, 318 $[M+2+Na]^+$, 320 $[M+4+Na]^+$ for $C_{13}H_9Cl_2N_3O$.

1–(4–Bromophenyl)–6–methyl–1*H*–pyrazolo[4,3–c]pyridin–4(5*H*)–one (**12k**): Brown solid; Yield 48%; mp = 270–271 °C; FTIR ($CHCl_3$) υ cm^{-1}3401,2917, 1669, 1494, 1349, 566; ^1H NMR ($CDCl_3$, 400 MHz): δ 10.63 (s, 1H), 8.31 (s, 1H), 7.67 (dd, *J* = 6.8, 1.9 Hz, 2H), 7.51 (dd, *J* = 6.9, 1.8 Hz, 2H), 6.35 (s, 1H), 2.41 (s, 3H); ^{13}C NMR ($CDCl_3$, 100 MHz): δ 160.4, 152.0, 144.6, 142.7, 138.2, 138.1, 132.7 (2C), 124.8 (2C), 121.4, 92.0, 19.8; MS (ESI) *m/z* 326 $[M+Na]^+$, 328 $[M+2+Na]^+$ for $C_{13}H_{10}BrN_3O$.

1–(3–Bromophenyl)–6–methyl–1*H*–pyrazolo[4,3–c]pyridin–4(5*H*)–one (**12l**): Brown solid; Yield 42%; mp = 278–281 °C; FTIR ($CHCl_3$) υ cm^{-1} 3419,2921, 1633, 750; ^1H NMR ($CDCl_3$, 400 MHz): δ 10.28 (s, 1H), 8.31 (s, 1H), 7.81 (br s, 1H), 7.58–8.55 (m, 2H), 7.41 (t, *J* = 8.0 Hz, 1H), 6.38 (s, 1H), 2.42 (s, 3H); ^{13}C NMR ($CDCl_3$, 100 MHz): δ 160.3, 146.4, 144.7, 142.8, 140.2, 138.2, 130.9, 130.8, 126.4, 123.1, 121.8, 91.9, 19.8; MS (ESI) *m/z* 326 $[M+Na]^+$, 328 $[M+2+Na]^+$ for $C_{13}H_{10}BrN_3O$.

1–(3–Fluorophenyl)–6–methyl–1*H*–pyrazolo[4,3–c]pyridin–4(5*H*)–one (**12m**): White; Yield 51%; mp = 230–232 °C; FTIR ($CHCl_3$) υ cm^{-1} 3429,2921, 1660, 1465, 789; ^1H NMR ($CDCl_3$, 400 MHz): δ 10.75 (s, 1H), 8.32 (s, 1H), 7.54–7.48 (m, 1H), 7.44 (d, *J* = 8.2 Hz, 1H), 7.39 (dd, *J* = 9.5, 2.0 Hz, 1H), 7.16–7.11 (m, 1H), 6.42 (s, 1H), 2.44 (s, 3H); ^{13}C NMR ($CDCl_3$, 100 MHz): δ 160.4, 144.7, 142.9, 140.6, 140.5, 138.2, 130.9, 130.8, 118.7, 118.7, 114.8, 114.6, 113.0, 111.0, 110.8, 92.0, 19.8; MS (ESI) *m/z* 265.98 $[M+Na]^+$ for $C_{13}H_{10}FN_3O$.

1–(3,4–Difluorophenyl)–6–methyl–1*H*–pyrazolo[4,3–c]pyridin–4(5*H*)–one (**12n**): White; Yield 41%; mp = 288–289 °C; FTIR ($CHCl_3$) υ cm^{-1} 3401,2918, 1673, 1469, 770; ^1H NMR (DMSO–d_6, 400 MHz): δ 11.33 (s, 1H), 8.24 (s, 1H), 7.81–7.76 (m, 1H), 7.68–7.61 (m, 1H),

7.54–7.52 (m, 1H), 6.52 (s, 1H), 2.25 (s, 3H); ^{13}C NMR (DMSO–d_6, 100 MHz): δ 159.2, 144.8, 144.7, 138.2, 120.4, 119.0, 118.8, 113.4, 113.2, 112.9, 102.1, 91.2, 19.4; MS (ESI) *m/z* 262 $[M+H]^+$ for $C_{13}H_9F_2N_3O$.

1–(3,5–Difluorophenyl)–6–methyl–1*H*–pyrazolo[4,3–c]pyridin–4(5*H*)–one (**12o**): Light brown; Yield 41%; mp = 281–284 °C; FTIR ($CHCl_3$) υ cm^{-1} 3435,2921, 1625, 747; ^{1}H NMR (DMSO–d_6, 400 MHz): δ 11.39 (s, 1H), 8.28 (s, 1H), 7.48 (d, J = 6.2 Hz, 2H), 7.39 (tt, J = 13.9, 2.3 Hz, 1H), 6.66 (s, 1H), 2.28 (s, 3H); ^{13}C NMR (DMSO–d_6, 100 MHz): δ 164.4, 164.3, 162.0, 161.8, 159.0, 145.0 (2C), 144.9, 141.4, 138.7 (2C), 113.4, 107.0, 106.9, 106.7, 103.3, 91.3, 19.4; MS (ESI) *m/z* 284.06 $[M+Na]^+$ for $C_{13}H_9F_2N_3O$.

1–(4–(*tert*–Butyl)phenyl)–6–methyl–1*H*–pyrazolo[4,3–c]pyridin–4(5*H*)–one (**12p**): Light brown; Yield 53%; mp = 246–247 °C; FTIR ($CHCl_3$) υ cm^{-1} 3435,2923, 1660, 1520, 779; ^{1}H NMR ($CDCl_3$, 400 MHz): δ 11.48 (s, 1H), 8.31 (s, 1H), 7.56–7.51 (m, 4H), 6.41 (s, 1H), 2.43 (s, 3H), 1.38 (s, 9H); ^{13}C NMR ($CDCl_3$, 100 MHz): δ 161.1, 151.1, 144.7, 142.5, 137.5, 136.6, 126.4 (2C), 123.0 (2C), 112.5, 92.4, 34.8, 31.3 (3C), 19.6 HRMS (ESI) *m/z* cacld for $C_{17}H_{19}N_3O$ $[M+Na]^+$: 304.1426, found: 304.1424.

4.5 *In silico* prediction of QED and ADMET properties

The quantitative estimation of drug likeness (QED) of synthesized fused–pyrazole derivatives were calculated. The molecular descriptors such as molecular weight (Mr), lipophilicity (ALOGP), number of hydrogen bond donors (HBDs), number of hydrogen bond acceptors (HBAs), polar surface area (PSA), number of aromatic ring (nAROM) and number of ratable bond (ROTBs) were used for QED calculation which were calculated using Dragon 5.4 software [29]. List of 105 toxicophores (notably nitro, conjugated nitrile, azido and thiocyanate) given by Bickerton *et al.* was used to identify the number of ALERTs [20]. Absorption, distribution,

metabolism, excretion (ADME) properties and carcinogenicity and mutagenicity were predicted using online admetSAR tool [23].

4.6 Biological studies

The synthesized fused–pyrazole derivatives were evaluated for their biological activity at ICMR–National AIDS Research Institute, Pune. The compounds were screened for cytotoxicity and anti–HIV activity using TZM–bl assay [30,31]. The anti-HIV potential of the most active lead(s) was further assessed on drug resistant viruses. The activity of the leads identified in screening assays was confirmed by assessing their anti–HIV–1 potential in Peripheral Blood Mononuclear Cells (PBMCs).

Cells

The TZM–bl cell line (genetically engineered HeLa cell line), obtained from the National Institutes of Health (NIH), USA under the AIDS Research Reference Reagent Program (NIH ARRRP) were used to assess the cytotoxicity and anti–HIV–1 activity. These cells are capable of expressing CD4, CXCR4, and CCR5 receptors that are necessary for HIV infection. Moreover, they are engineered with Tat–responsive reporter genes like firefly luciferase (Luc) and *Escherichia coli* β–galactosidase enzymes downstream of HIV–1 LTR. The cells were maintained in Dulbecco's modified Eagle's medium (DMEM; Gibco–Invitrogen, USA) supplemented with 10% fetal bovine serum (FBS; Moregate Biotech, Australia), penicillin 100 U/mL and streptomycin 100 mg/mL (Gibco–Invitrogen, USA) and 25 mM HEPES buffer solution (Gibco–Invitrogen, USA). The cell culture was incubated at 37 °C in a humidified 5% CO_2 atmosphere and used when 80% confluency was achieved [32].

Viruses

For the assessment of anti–HIV1 activity, primary isolates of HIV–1 *i.e.* HIV–1_{VB59} (CCR5 tropic, Subtype C from India) and HIV–1_{UG070} (CXCR4 tropic, Subtype D from Uganda) were used. The activity of the lead compound obtained in the primary screening was tested against HIV-1 92/BR/018 (Brazilian isolate, deposited through UNAIDS network "HIV-1 isolation and characterization"), NIH-119 virus (NVP resistant isolate, catalog number- 1392) [33] procured through NIH ARRRP and a HIV-1drug resistant primary isolate (NARI-DR) primary isolate isolated at ICMR-NARI, Pune. The viruses were grown in the PHA–P (Sigma–Aldrich, USA, 5 µg/ml) activated PBMCs derived from healthy donors and maintained in complete growth medium *i.e.* RPMI 1640 supplemented with 5U/mL IL2 and 10% FBS. The viral growth was quantified by detection of HIV–1 p24 antigen (Advanced Bioscience Laboratories, Inc., USA). The cell–free culture supernatants of viruses were collected by centrifugation, filtered and stored in aliquots at –70°C. The virus stocks were titrated in TZM–bl cells and $TCID_{50}$ (50% Tissue culture infective dose) of each virus stock was determined [34].

Cytotoxicity assay

In brief, the cultured TZM–bl (10^4 cells/well) cells were seeded in microplates for overnight incubation at 37°C in a humidified 5% CO_2 atmosphere. Followed by serial two-fold dilutions of the compounds and drug control (AZT) were prepared and added onto the cells. After incubation of 48 h at the same conditions, the cell viability was determined using MTT (3–(4,5-dimethyl thiazole–2–yl)–2,5–diphenyl tetrazolium bromide) (Sigma Aldrich, Inc., USA). The results were expressed as CC_{50} (The concentration at which 50% cells are viable) which was calculated by non–linear regression curve fitting.

Cell associated HIV–1 assay

To determine the anti-HIV1 activity, microplates were pre–seeded with TZM–bl cells (10^4 cells/well) and next day were used for cell associated assay. Cells were first infected with pre–titrated virus stocks of HIV–1_{VB59} or HIV–1_{UG070} and incubated for 2h. Serial two fold dilutions of sub–toxic concentrations of the compound/drug control (AZT) were prepared added onto the infected cells, and plate was incubated for 48 h. The untreated TZM–bl cells infected with the respective viruses as well as non–infected cells were included as controls. After 48 h, the Britelite plus reagent (Perkin Elmer, USA), a substrate to detect luciferase gene product, was added and the Relative Luminescence Units (RLU) were measured using Luminometer (Victor 3, Perkin Elmer, USA). The percent inhibition was calculated and the results were expressed as IC_{50} value (concentration inhibiting 50% of the virus) using LUC software (version 04.4). Therapeutic indices (TI= CC_{50}/IC_{50}) were calculated and compared with drug control. The compound that exhibited highest TI was tested at least in three independent assays. Furthermore, the active lead compound was tested against Subtype B primary isolate 92/BR/018 and drug resistant isolates; NIH-119 virus and NARI-DR. NVP and AZT were used as controls in these assays.

Confirmatory assays in PBMCs

The cytotoxicity and anti–HIV–1 activity of the lead compound **12c** was also assessed in PBMCs which are the primary targets of HIV–1. In brief, PBMCs (0.2×10^6 cells/ well) activated with PHA–p (5μg/mL) and IL–2 (5U/mL) were added to serial two-fold dilution of the lead compound **12c** and incubated at 37°C in 5% CO2 atmosphere for 5 days. The viability of the cells was measured by MTT assay and CC_{50} value was calculated accordingly. Subsequently, sub–toxic concentrations were used in determining the anti–HIV–1 activity against R5 tropic HIV–1_{VB51} as described earlier [30].

Time-of-addition (ToA) experiment

The ToA assay was performed as described previously [35]. TZM-bl cells (10^4 cells/well) were seeded in 96-well plates. After overnight incubation, cells were infected with HIV-$1NL_{4.3}$ ($400TCID_{50}$ mL) in complete DMEM supplemented with 25 mg/mL DEAE-dextran (Sigma-Aldrich, USA). Known anti-retrovirals, Dextran sulfate (DS), AZT, NVP, Raltegravir (RAL), Ritonavir (RTV) and lead compound **12c** were used at concentrations five-folds of their IC_{50} values. The prepared dilutions were added at different time points (0, 1, 2, 3, 4, 6, 8, 10, 18 and 24 h) post infection. Luciferase activity was measured after 48 h post infection. The experiments were carried out in triplicate and the mean±SD were calculated.

HIV–1 Reverse transcriptase inhibition assay

The potential of the lead compound to block the HIV–1 reverse transcriptase was also assessed in enzymatic assay using the HIV–1 reverse Transcriptase assay kit (Roche) according the manufacturer's instructions. Another compound (**12a**) which had shown less activity in the TZM–bl assay was also included in the assays. Briefly, the compound dilutions were incubated with the HIV–1 RT and template nucleotide mix for 1h. Subsequently, this was transferred to the streptavidin coated micro well plates and further incubated for 1h to allow the binding of the biotin, DIG labeled template primer complex to the streptavidin plate. Sufficient washing was performed to remove any unbound template. The HRP enzyme conjugate was added and incubated for 1h. The absorbance was measured at 405 nm (reference at 490 nm) after addition of substrate. The IC_{50} values were calculated using non-linear regression curves generated based on the percentage inhibition (calculated by comparing with the controls containing no inhibitors) of the drug tested at three different concentrations. Three independent assays were used to determine mean IC_{50} values. AZT and NVP were used as controls in the assays.

4.7 Molecular Docking

The crystal structure of HIV-1 reverse transcriptase was obtained from the Brookhaven Protein Data Bank (http://www.rcsb.org/) (entry code 3m8p) for molecular docking study. All water molecules and co-crystallized ligand were removed before docking calculations. The 3D atomic coordinates of the ligands were created from molecular connectivity via distance geometry and confomer ensembles using a multi-objective genetic algorithm incorporated in command line tool Balloon [36]. The protein structure was prepared using AutoDockTools [37]. The blind docking calculations were performed using Blind Docking Web Server (http://bio-hpc.ucam.edu/aquiles/). The docking studies of all the compounds in the NNBP were performed using Qvina-W [38]. A 25×25×25 Å size grid centered on coordinates x=49.347, y=63.892 and z=17.144 were used for docking calculations. The protein-ligand interactions were studied using Protein-Ligand Interaction Profiler (PLLIP) [39] and results were viewed using PyMol [40] molecular viewer.

CONFLICT OF INTEREST

The authors confirm that this article content has no conflict of interest.

5 ACKNOWLEDGEMENTS

Authors are thankful to the Director, NIPER and Director, NARI for supporting this work. Authors acknowledge the Department of Biotechnology (DBT) (grant no. BT/PR5634/MED/29/623/2012) and Indian Council of Medical Research (ICMR) (grant no. 5/7/827/12–RCH), Government of India for the financial support to this project.

6 REFERENCES

[1] WHO. HIV/AIDS. http://www.who.int/mediacentre/factsheets/fs360/en/, (Accessed on October 15, 2018).

[2] UNAIDS. HIV/AIDS. http://www.unaids.org (Accessed on October 15, 2018).

[3] I. P. Singh, H. S. Bodiwala, Recent advances in anti–HIV natural products, Nat. Prod. Rep. 27 (2010) 1781–1800.

[4] A. H. Abadi, A. A. H. Eissa, G. S. Hassan, Synthesis of novel 1, 3, 4–trisubstituted pyrazole derivatives and their evaluation as antitumor and antiangiogenic agents, Chem. Pharm. Bull. 51 (2003) 838–844.

[5] R. J. Flower, The development of COX2 inhibitors, Nat. Rev. Drug Discovery 2 (2003) 179–191.

[6] M. Wasil, M. Harris, B. Henderson, Antioxidant activity of dipyrone: relationship to its anti–inflammatory and analgesic activity, Pharmacol. Commun. 1 (1992) 337–344.

[7] N. K. Terrett, A. S. Bell, D. Brown, P. Ellis, Sildenafil (VIAGRATM), a potent and selective inhibitor of type 5 cGMP phosphodiesterase with utility for the treatment of male erectile dysfunction, Bioorg. Med. Chem. Lett. 6 (1996) 1819–1824.

[8] Y. Xing, J. Zuo, P. Krogstad, M. E. Jung, Synthesis and Structure–Activity Relationship (SAR) studies of novel pyrazolopyridine derivatives as inhibitors of enterovirus replication, J. Med. Chem. 61 (2018) 1688–1703.

[9] M. A. M. Abdel Reheim, S. M. Baker, Synthesis, characterization and in vitro antimicrobial activity of novel fused pyrazolo[3,4–c]pyridazine, pyrazolo[3,4–d]pyrimidine, thieno[3,2–c]pyrazole and pyrazolo[3',4':4,5]thieno[2,3–d]pyrimidine derivatives, Chem. Cent. J. 11 (2017) 112.

562 [10] L.–G. Yu, T.–F. Ni, W. Gao, Y. He, Y.–Y. Wang, H.–W. Cui, C.–G. Yang, W.–W. Qiu,
563 The synthesis and antibacterial activity of pyrazole–fused tricyclic diterpene derivatives,
564 Eur. J. Med. Chem. 90 (2015) 10–20.
565 [11] D. Anand, P. K. Yadav, O. P. Patel, N. Parmar, R. K. Maurya, P. Vishwakarma, K. S. Raju,
566 I. Taneja, M. Wahajuddin, S. Kar, P. P. Yadav, Antileishmanial activity of
567 pyrazolopyridine derivatives and their potential as an adjunct therapy with miltefosine, J.
568 Med. Chem. 60 (2017) 1041–1059.
569 [12] I. F. Nassar, A. F. El Farargy, F. M. Abdelrazek, Synthesis and anticancer activity of some
570 new fused pyrazoles and their glycoside derivatives, J. Heterocyclic Chem. 55 (2018)
571 1709–1719.
572 [13] G. Bertuzzi, E. Locatelli, D. Colecchia, P. Calandro, B. Bonini, J. Chandanshive, A.
573 Mazzanti, P. Zani, M. Chiariello, M. C. Franchini, Straightforward synthesis of a novel
574 ring–fused pyrazole–lactam and *in vitro* cytotoxic activity on cancer cell lines, Eur. J. Med.
575 Chem. 117 (2016) 1–7.
576 [14] G. N. Tageldin, S. M. Fahmy, H. M. Ashour, M. A. Khalil, R. A. Nassra, I. M. Labouta,
577 Design, synthesis and evaluation of some pyrazolo[3,4–d]pyrimidines as anti–
578 inflammatory agents, Bioorg. Chem. 78 (2018) 358–371.
579 [15] J. V. Faria, P. F. Vegi, A. G. C. Miguita, M. S. Dos Santos, N. Boechat, A. M. R.
580 Bernardino, Recently reported biological activities of pyrazole compounds, Bioorg. Med.
581 Chem. 25 (2017) 5891–5903.
582 [16] D. Raffa, B. Maggio, M. V. Raimondi, S. Cascioferro, F. Plescia, G. Cancemi, G. Daidone,
583 Recent advanced in bioactive systems containing pyrazole fused with a five membered
584 heterocycle, Eur. J. Med. Chem. 97 (2015) 732–746.

[17] T. J. Tucker, J. T. Sisko, R. M. Tynebor, T. M. Williams, P. J. Felock, J. A. Flynn, M.–T. Lai, Y. Liang, G. McGaughey, M. Liu, Discovery of 3–{5–[(6–amino–1 H–pyrazolo [3, 4–b] pyridine–3–yl) methoxy]–2–chlorophenoxy}–5–chlorobenzonitrile (MK–4965): a potent, orally bioavailable HIV–1 non–nucleoside reverse transcriptase inhibitor with improved potency against key mutant viruses, J. Med. Chem. 51 (2008) 6503–6511.

[18] D.–S. Su, J. J. Lim, E. Tinney, B.–L. Wan, M. B. Young, K. D. Anderson, D. Rudd, V. Munshi, C. Bahnck, P. J. Felock, Biaryl ethers as novel non–nucleoside reverse transcriptase inhibitors with improved potency against key mutant viruses, J. Med. Chem. 52 (2009) 7163–7169.

[19] M. M. Savant, K. D. Ladva, A. B. Pandit, Facile synthesis of highly functionalized novel pyrazolopyridones using oxoketene dithioacetal and their anti–HIV activity, Synth. Commun. 48 (2018) 1640–1648.

[20] G. R. Bickerton, G. V. Paolini, J. Besnard, S. Muresan, A. L. Hopkins, Quantifying the chemical beauty of drugs, Nat. Chem. 4 (2012) 90–98.

[21] S. Gupta, S. Kumar, N. Jariwala, D. Bhadane, K. K. Bhutani, S. Kulkarni, I. P. Singh, *In silico* prioritization, synthesis and *in vitro* evaluation of tembamide analogs for anti–HIV activity, Lett. Drug Des. Discovery 14 (2017) 1455–1464.

[22] S. Kumar, S. Gupta, S. Gaikwad, L. Abadi, L. Bhutani, S. Kulkarni, I. Singh, Design, synthesis and in vitro evaluation of novel anti–HIV 3–pyrazol–3–yl–pyridin–2–one analogs, Med. Chem. (2018) doi: 10.2174/1573406414666181106125539.

[23] F. Cheng, W. Li, Y. Zhou, J. Shen, Z. Wu, G. Liu, P. W. Lee, Y. Tang, admetSAR: A comprehensive source and free tool for assessment of chemical ADMET properties., Chem. Inf. Mod. 52 (2012) 3099–3105.

608 [24] Drug bank. https://www.drugbank.ca/drugs (Accessed on October 15, 2018).
609 [25] E. Walton, J. Rodin, C. Stammer, F. Holly, Synthesis of L–valyl–L–tryosyl–L–tyrosyl–L–
610 isoleucyl–L–histidyl–L–prolyl–L–phenylalanine methyl ester dihydrochloride, J. Org.
611 Chem. 26 (1961) 1657–1658.
612 [26] H. H. Showalter, T. H. Haskell, Functionalization of substituted 2–(1*H*) pyridones. I. A
613 novel synthesis of □–arylgyloxylates and related systems, J. Het. Chem. 18 (1981) 367–
614 370.
615 [27] D. Tomasik, P. Tomasik, R. A. Abramovitch, Friedländer condensation of 1*H*–pyrazolin–
616 5–ones with *o*–aminobenzaldehydes. Synthesis of 1H–pyrazolo [3, 4–□] quinolines, J.
617 Heterocycl. Chem. 20 (1983) 1539–1543.
618 [28] R. Esnouf, J. Ren, C. Ross, Y. Jones, D. Stammers, D. Stuart, Mechanism of inhibition of
619 HIV-1 reverse transcriptase by non-nucleoside inhibitors, Nat. Struct. Mol. Biol. 2 (1995)
620 303–308.
621 [29] I. V. Tetko, J. Gasteiger, R. Todeschini, A. Mauri, D. Livingstone, P. Ertl, V. A. Palyulin,
622 E. V. Radchenko, N. S. Zefirov, A. S. Makarenko, Virtual computational chemistry
623 laboratory–design and description, J. Comput.–Aided Mol. Des. 19 (2005) 453–463.
624 [30] V. Murugesan, N. Makwana, R. Suryawanshi, R. Saxena, R. Tripathi, R. Paranjape, S.
625 Kulkarni, S. B. Katti, Rational design and synthesis of novel thiazolidin–4–ones as non–
626 nucleoside HIV–1 reverse transcriptase inhibitors, Bioorg. Med. Chem. 22 (2014) 3159–
627 3170.
628 [31] M. S. Said, A. A. Chinchansure, L. Nawale, A. Durge, A. Wadhwani, S. S. Kulkarni, D.
629 Sarkar, S. P. Joshi, A new butenolide cinnamate and other biological active chemical
630 constituents from *Polygonum glabrum*, Nat. Prod. Res. 29 (2015) 2080–2086.

[32] C. A. Derdeyn, J. M. Decker, J. N. Sfakianos, X. Wu, W. A. O'Brien, L. Ratner, J. C. Kappes, G. M. Shaw, E. Hunter, Sensitivity of human immunodeficiency virus type 1 to the fusion inhibitor T–20 is modulated by coreceptor specificity defined by the V3 loop of gp120, J. Virol. 74 (2000) 8358–8367.

[33] D. Richman, C. K. Shih, I. Lowy, J. Rose, P. Prodanovich, S. Goff, J. Griffin, Human immunodeficiency virus type 1 mutants resistant to nonnucleoside inhibitors of reverse transcriptase arise in tissue culture, Proc. Natl. Acad. Sci. USA 88 (1991) 11241–11245.

[34] M. Cornelissen, G. Kampinga, F. Zorgdrager, J. Goudsmit, Human immunodeficiency virus type 1 subtypes defined by env show high frequency of recombinant gag genes. The UNAIDS Network for HIV isolation and characterization, J. Virol. 70 (1996) 8209–8212.

[35] D. Daelemans, R. Pauwels, E. De Clerq, C. Pannecouque, A time-of-drug addition approach to target identification of antiviral compounds, Nat. Protoc. 6 (2011) 925-933.

[36] J. S. Puranen, M. J. Vainio, M. S. Johnson, Accurate conformation-dependent molecular electrostatic potentials for high-throughput in silico drug discovery, J. Comput. Chem. 31 (2010) 1722–1732.

[37] G. M. Morris, R. Huey, W. Lindstrom, M. F. Sanner, R. K. Belew, D. S. Goodsell, A. J. Olson, Autodock4 and AutoDockTools4: automated docking with selective receptor flexiblity, J. Comput. Chem. 16 (2009) 2785–2791.

[38] N. M. Hassan, A. A. Alhossary, Y. Mu, C. Kwoh, Protein-ligand blind docking using QuickVina-W with inter-process spatio-temporal integration, Sci. Rep. 7 (2017).

[39] S. Salentin, S. Schreiber, V. J. Haupt, M. F. Adasme, M. Schroeder, PLIP: fully automated protein–ligand interaction profiler, Nucleic Acids Res. 43 (2015) W443–W447.

654 [40] W. L. DeLano, Pymol: An open-source molecular graphics tool, CCP4 Newsletter On
655 Protein Crystallography 40 (2002) 82–92.

Highlights

- Novel Pyrazolo[4,3–c]pyridin–4–one derivatives designed and synthesized
- QED and *in silico* ADMET properties predicted
- Evaluated for anti-HIV-1 activity
- Lead compound was further confirmed by PBMC assay
- The compound was shown to act through inhibition of reverse transcriptase